Asian Journal of Chemistry; Vol. 33, No. 11 (2021), 2857-2863

ASIAN JOURNAL OF CHEMISTRY

https://doi.org/10.14233/ajchem.2021.23501

Graphene Oxide Nanoparticles Decorated Pencil Lead as Urea Sensing Electrode

SARAVJEET SINGH[1], MINAKSHI SHARMA[2] and GEETA SINGH[1,*]

[1]Department of Biomedical Engineering, Deenbandhu Chhotu Ram University of Science and Technology, Murthal-131039, India
[2]Department of Zoology, Maharishi Dayanand University, Rohtak-124001, India

*Corresponding author: E-mail: geetasingh.bme@dcrustm.org

Received: 27 August 2021; *Accepted*: 6 October 2021; *Published online*: 20 October 2021; AJC-20575

In present study, a low-cost and steady electrochemical biosensor has been developed based on graphene oxide nanoparticles (GONPs), electrodeposited on the pencil lead electrode (PLE). The physical and morphological studies revealed the nano-scale range of GONPs that has an average grain size/layer thickness of 2.27 nm and agglomeration size of 90-120 nm. Urease enzyme was immobilized on PLE/GONPs electrode after surface treatment with 1-ethyl-3-(3-dimethylaminopropyl)carbodiimide hydrochloride (EDC)/*N*-hydroxysuccinimide (NHS) to impart stable peptide bond. Scanning electron microscopy (SEM) studies demonstrate the difference between unmodified and modified PLE electrodes and depict the spherical, circular and flaky-like morphology. The electrochemical analysis of urea considerably improved on the PLE/GONPs/Ur compared to the untailored PLE electrode. The reported urea biosensor operated in a linear dynamic range between 0.30-50 mM that attained a recognition limit of 0.06 mM and exhibited an advanced exposure sensitivity of 0.814 μA mM^{-1} cm^{-2}.

Keywords: Urea, Sensor, Nanoparticles, Pencil lead electrode, Graphene oxide.

INTRODUCTION

Biosensors and biosensing electrodes in particular are an analytical tool that transduces the biological response into electrical response [1]. The pencil lead electrode (PLE) [2] is a rising biosensor electrode that substitutes the usual carbon and other metallic-based electrodes during this current epoch. The critical composition of PLE is graphite, a most stable structure of carbon obtainable in granite ores similar to coal. Moreover, as compared to carbon allotropes and other predictable metal electrodes, PLE, worked as a disposable electrode, expanded much contemplation among the electrochemical group for its profusion at minimal price through a variety of attractive possessions like mechanical stiffness, chemical limpness, short backdrop current, extensive potential window, analytical adsorption, simplicity of tininess and alteration. The sp^2 hybridized carbons of graphite allotrope are constant to the high-quality adsorption and superior conductivity. Thus, graphite compound layers on the usual electrodes are utilized for the voltammetric verification of geno-toxic nitro composite, organic composite, along with nucleic acids [3]. Fascinatingly, pencil lead electrodes (PLEs) are distinctly capable of effortlessly renewing shells compared to the rigorous polish process required for the usual electrodes [4-7]. Pencil lead electrodes (PLEs) acquiesce of renewing surfaces improves reproducibility for the analyses. Nanoparticles modified PLEs result in significantly changed properties such as enhanced redox potential window, sensitivity and selectivity [1,8].

In general, urea is generated inside the liver and exorcising like urine through the kidneys. Moreover, a small quantity of urea is excreted within sweat by the human body [9,10]. Urea biosensors are functional to envisage the character and origin of renal failure and be necessary for malfunctioning observations of the kidney. Peculiarly, soaring urea intensity inside the blood is a burly sign of prejudice kidney task or malfunction. The soaring or small intensity of urea absorption is a sign of numerous metabolic aberration, kidney collapse, liver malfunction, gastrointestinal hemorrhage, urinary strip impediment, nephritic disease, distress and cachexia [11]. In human being, excess proteins create amino acids following hydrolysis in the digestive method. The liver is the organ where the primary metabolic reaction occurs. Urea that unswervingly accomp-

lishes the blood flow from the kidneys is also egested in urine [12].

The ordinary urea absorption varies in the person's body from 2.5 mM to 7.8 mM [9-11,13]. With the deviation in normal urea concentration, kidney infection and hyper-ammonemia possibly arise. The existence of urea in the surroundings is also a subject of immense distress for environment preservation and individual healthiness guard. Due to its comparatively superior water-soluble nature, a significant quantity of the functional urea herbicides is swabbed out from the ecosystem. It can contaminate the exterior and the groundwater into which it depletes. It is consequently necessary to investigate urea in the surroundings, ingestion system of water and foodstuff. The electrochemical examination has intrinsic benefits of ease, elevated sensitivity and comparatively less price over complicated conventional techniques like soaring recital liquid chromatography and similar techniques [14-16].

The majority of the urea sensing techniques are based on the principle of biosensing, which employs the urease enzyme as an intellectual ingredient. Zhu *et al.* [17] presented an online urea detection method by developing zeolitic imidazolate framework. This optical biosensor made use of the principle of change in refractive index as a result of the formation of the substrate-enzyme complex. The biosensor thus developed has a detection limit of 0.1 mM and a linear range of 1^{-10} mM [17]. A novel biosensor comprising glassy carbon electrode (GCE) and nanocomposite of zinc phthalocyanine/GO (ZnPh/GO) was developed by Selvarajan *et al.* [18] through drop-casting and sonochemical methods. The biosensor responded with a linear range of 0.40 to 22 μM with LOD of 0.034 μM]. Evanescent wave absorption (EWA) based urea biosensor was fabricated by Botewad *et al.* [19] by layering cladding of an optical fiber with polyaniline-zinc oxide (PANI-ZnO). The sensor responded linearly in range of 10 nM -1 M and showed stability of 40 days without any significant loss of activity. Amin *et al.* [20] proposed a novel electrochemical enzymatic biosensor employing GCE decorated with nano-needles of nickel cobalt oxide ($NiCo_2O_4$). This GCE modified electrode responded linearly in the range of 0.01 to 5.0 mM with LOD of 1 μM. The sensor was highly selective in the presence of analytes like glucose, ascorbic acid and uric acid.

In present study, graphene oxide nanoparticles (GONPs) comprise and are utilized to modify the PLE nature for application in urea biosensors. The utilization of GONPs between the PLE and the urease coating is predictable to adsorb and strengthen stoutly with ultra-high sensitivity; this anticipation is found due to the existence of sizeable functional grouping with improved electron relocate possessions.

EXPERIMENTAL

Urease from *Canavalia ensiformis* (Jack bean) was procured from Sigma-Aldrich, USA. Sodium nitrate, sulphuric acid, $KMnO_4$, hydrogen peroxide and hydrogen chloride obtained from Qualigens Fine Chemicals, Mumbai that were employed for synthesis process. A graphite pencil-6HB (Make: Apsara, Hindustan Pencils Pvt. Ltd) used as carbon precursor with a graphite bar of 2.0 mm diameter. Distilled water (ohmic resistance of 1.9×10^{-5} for every ohm) was used during the entire investigation.

Instruments: Autolab PGSTAT204 electrochemical work station (Metrohm Autolab B.V., The Netherlands) with NOVA software was used for the electrochemical studies. Scanning electron microscopy (LEO 435VP LEO), UV-vis spectrophotometer (Shimadzu, UV-2450), FTIR (Perkin Elmer FRONTIER) and X-ray diffractometer (Rigaku Ultima, IV) were utilized for the characterization of samples at various stages of PLE modification.

Synthesis process of nanoparticles of graphene oxide (GONPs): GONPs were synthesized by modified Hummer's process [21-23] with minor alterations. For this, 6HB lead pencil was employed as precursor material. The pencil lead was transformed into powdered form by using a pestle and mortar. The above-transformed powder of pencil lead was mixed with sodium nitrate in a known amount in an Erlenmeyer flask of 1000 mL with dropwise addition of concentrated sulfuric acid. After that potassium permanganate was added leisurely while stirring magnetically for a couple of days at a temperature of < 20 ºC. After that, 250mL of dilute sulphuric acid (5% v/v) was supplemented in the mixture and heated on a hot plate at 98 ºC. Once it attained the required temperature, it was heated again at that temperature for 2 h and then cooled to 60 ºC. Finally, the reaction was completed by adding H_2O_2 (7.50 mL), with continuous stirring for another 2 h. The blend obtained was ultracentrifuged at 6000 RCF for 15 min to accumulate suspensions at the bottom and consequently was rinsed 10 times and 5 times with a solution of hydrogen peroxide and hydrochloric acid, respectively. At last, the mixture was neutralized by washing with deionized water several times. Finally, the nanomaterial obtained was vacuum dried overnight for dehydration, resulting in light brown coloured powder called GONPs. The schematic process is shown in Fig. 1.

Grafting of GONPs on PLE (PLE/GONPs): GONPs were grafted on pencil lead electrode using electrodeposition techniques through cyclic voltammetry. For this, pencil of 6B hardness was carved to 3 cm for the exposure of graphite rod for electric connections. Prepared GONPs (2 mg) were dispersed in 25 mL of 0.1 M HCl under continuous stirring at 95 ºC. The dispersed GONPs were electrodeposited on PLE through cyclic voltammetry by executing 22 cycles of polymerization in a voltage range of -0.1-0.9 V with scanning at 20 mV/S.

Immobilization of urease enzyme on PLE/GONPs: The surface of PLE/GONPs electrode was immobilized using the urease enzyme. For this, the electrode was pretreated with a solution of 1-ethyl-3-(3-dimethylaminopropyl)carbodiimide hydrochloride (EDC) and *N*-hydroxysuccinimide (NHS) for 30 min to induce carbodiimide activation chemistry for enhancing the immobility of the enzyme [24-26]. After that the electrode was dipped in urease solution (4 mg/mL) overnight for the coupling of urease on the working electrode.

Characterization methods for GoNPs and biosensing electrode: X-ray diffraction was utilized for analyzing the phase separation and grain size of pencil lead electrode (PLE) and GONPs. The grain size was calculated using the Scherrer's equation [27]:

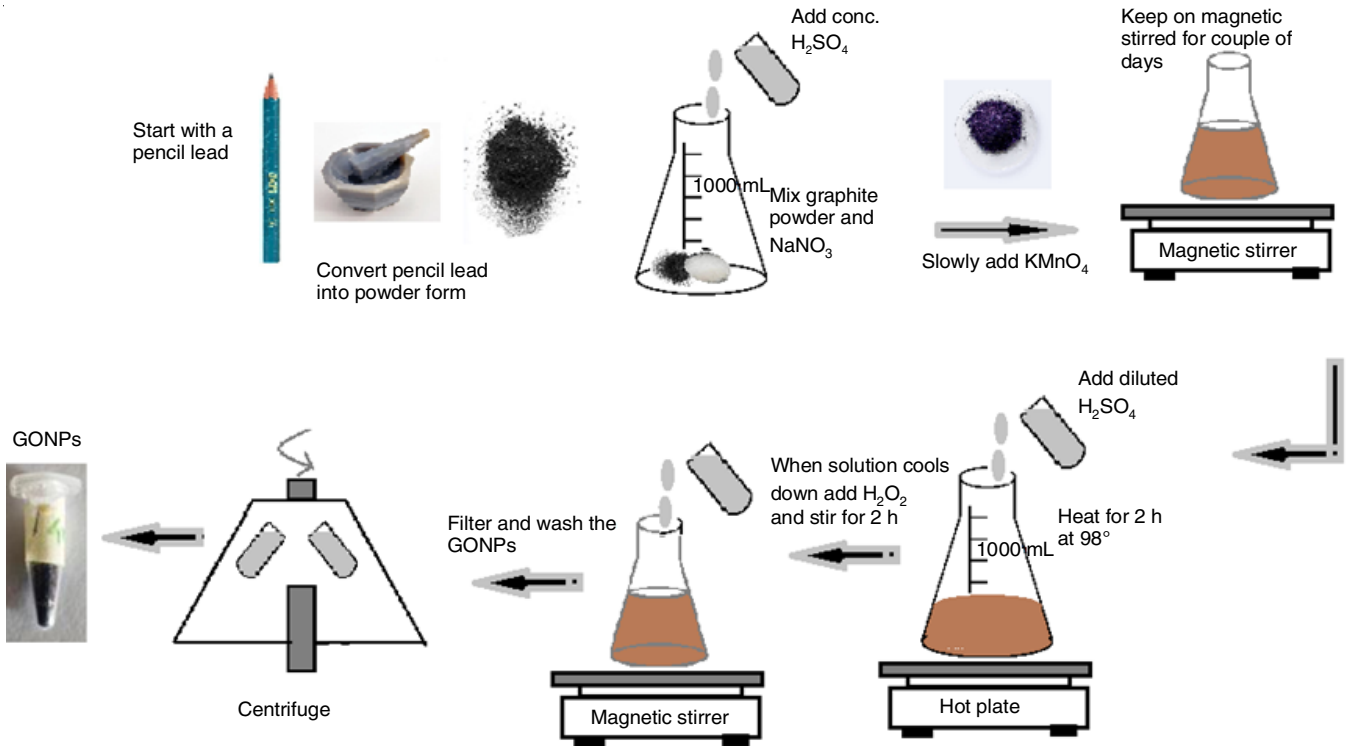

Fig. 1. Schematic route of graphene oxide nanoparticles (GONPs) synthesis

$$D = \frac{0.89\lambda}{\beta \cos\theta} \quad (1)$$

where λ is wavelength (Cu*K*α), β is full width at half maximum (FWHM) and θ is diffraction angle.

SEM analysis: Morphology of PLE and GONPs was studied using scanning electron microscopy (SEM). The samples were prepared by dispersing PLE and GONPs in ethanol ultrasonically for 20 min. A dilute suspension was dropped on the platinum grid to make the sample conducting. A 20 kV accelerating voltage was used for taking the images at different magnifications.

FTIR analysis: FTIR was done using KBr pellets on Perkin-Elmer RZX spectrometer in the spectral range of 4000-450 cm^{-1}. Each sample was scanned thrice. A Shimadzu spectrophotometer model UV-1200 was used for UV spectra analysis with wavelength of 200-600 nm.

Electrochemical studies: Autolab, PGSTAT204 electrochemical work station (MetrohmAutolab B.V., The Netherlands), was utilized for examining the electrochemical response of the urease immobilized PLE/GONPs at various steps of fabrication. Measurements were executed in an electrolytic solution containing 1 M KCl dilution and 3 mM potassium ferric cyanide as a redox mediator in boric acid buffer (20 mM). All the samples were performed in phosphate buffer saline (PBS) for maintaining the pH to 7. Each sample was scanned thrice with a scan rate of 0.03 V/s. The raw data obtained was analyzed using Nova software.

RESULTS AND DISCUSSION

XRD studies: X-ray diffractograms of pencil lead electrode (PLE) and graphene oxide nanoparticles (GONPs) are shown in Fig. 2a and b, respectively. Sharp peaks at 54.7º (004) and 44.8º (100) in Fig. 2a indicate that the structure of PLE is highly crystalline [27,28]. Further, peak at 26.5º (002) with *d*-spacing of 0.15 nm signifies highly ordered carbon structure of graphene [29]. The characteristic 001 peak of graphene oxide is seen at 10.7º (Fig. 2b) with a *d*-spacing of 0.75 nm is due to oxygen containing functional groups that helps in dispersion of GONPs with solvent to exfoliation state [30].

Grain size: The grain size of GONPs was calculated using the Scherer's equation. For this, the Gaussian fit was applied in Origin pro 9 software for calculating full width at half-maximum (FWHM) as shown in Fig. 2c. The obtained value of FWHM and 2θ was then used to calculate grain size. The average grain size was found to be 2.27 nm.

FTIR studies: Fig. 3a & b show the FTIR spectrum of PLE and GONPs, respectively. The broad and sharp peak at 3432 and 1628 cm^{-1}, respectively, is due to stretching and bending vibration of OH molecule because of adsorption of water molecules on graphene oxide, indicating strong hydrophilicity of GONPs [31]. The peaks at 2926 and 2853 cm^{-1} are due to symmetric and asymmetric stretching vibration of methylene (CH_2) group [32]. The peak at 1728 and 742 cm^{-1} corresponds to the stretching vibration of C-C and C=O of carboxyl and carbonyl group [33,34]. Lastly, the peaks at 1387 and 1087 cm^{-1} are due C-O stretching vibrations of epoxides and alcohols, respectively [31,33]. The oxidation of graphene is confirmed by existence of these oxygen containing functional groups. The hydrophilic nature of GONPs is affirmed by the formation of hydrogen bond between graphene and water molecules.

UV-visible studies: Shimadzu UV-250 spectrophotometer was utilized for analyzing the structure using UV-vis spectro-

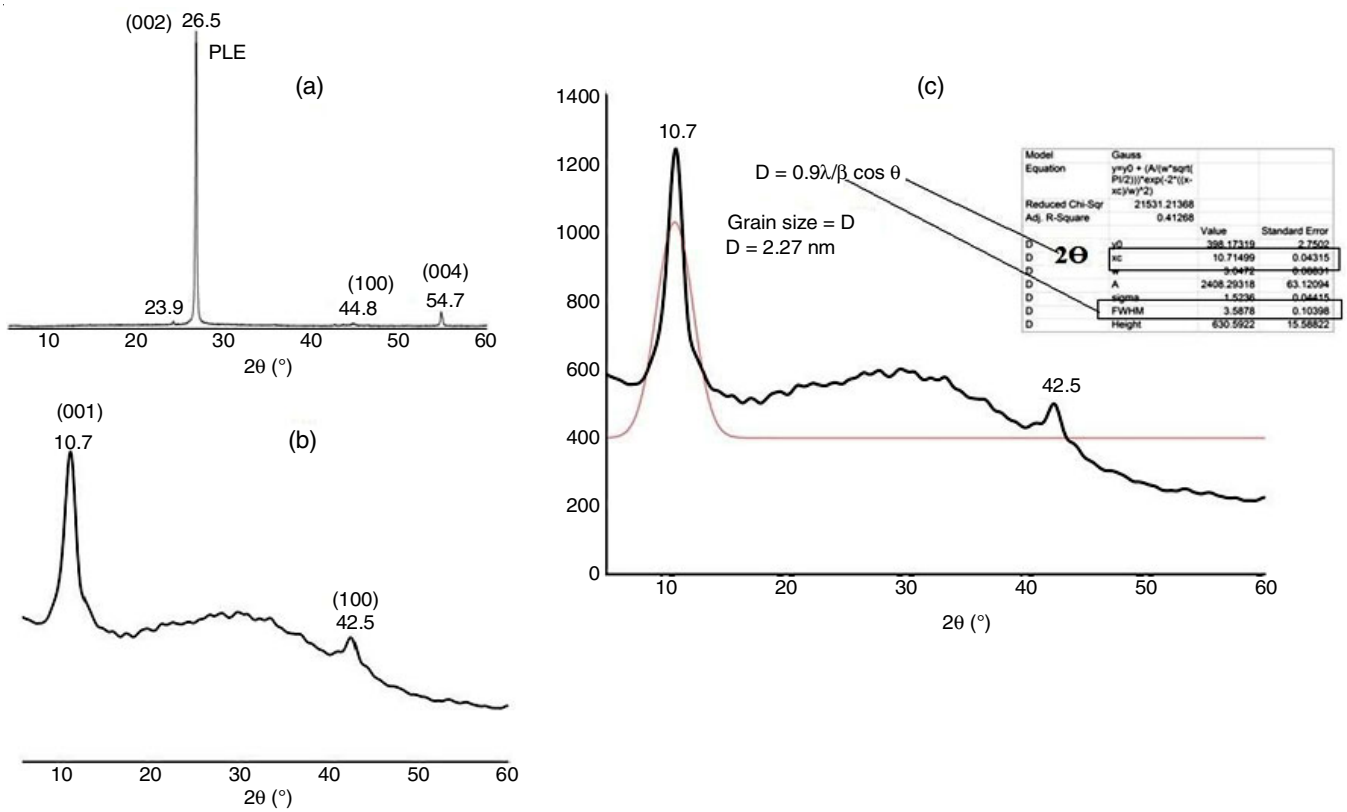

Fig. 2. (a-b) X-ray diffraction of PLE and GO-NPs (c) Gauss fitting for grain size calculation

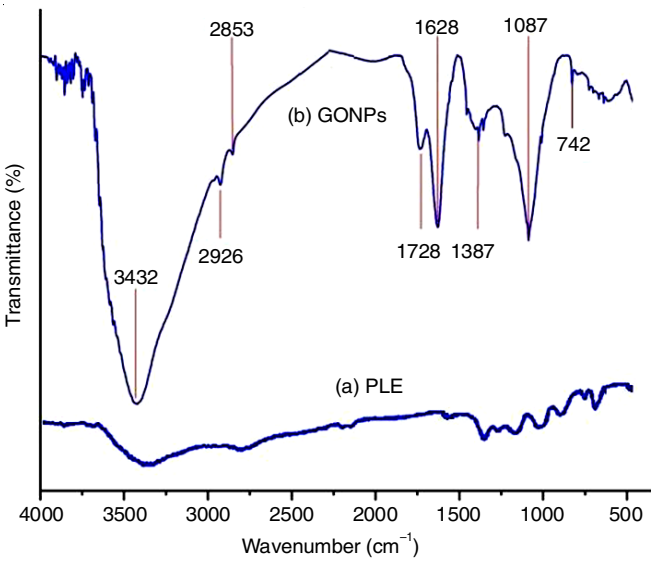

Fig. 3. FTIR spectrum of (a) PLE (b) GONPs

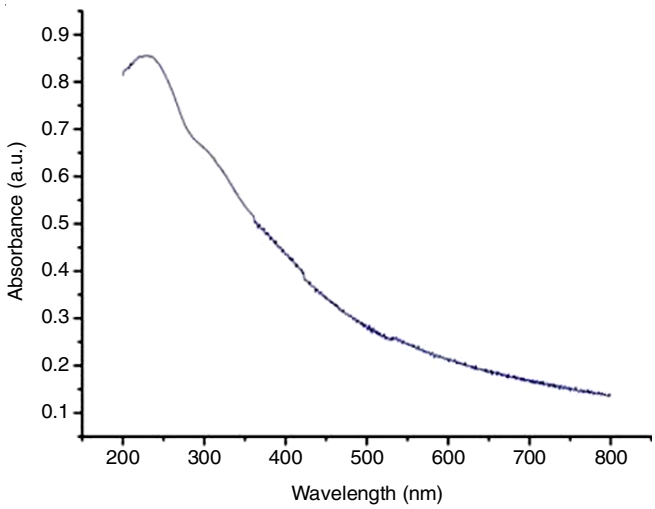

Fig. 4. UV-vis spectrograph of graphene oxide nanoparticles (GONPs)

scopy. For this, GONPs were liquefied in distilled water (0.1 mg/mL) and then dilution was examined using a UV-vis spectrophotometer between 200-800 nm. The maximum absorbance at 0.856 was observed at 230 nm (Fig. 4). This may be due to the π-π* transition of the atomic C-C bonds. Further, a shoulder peak around 300 nm was also observed, which maybe because of the n-π* transition of aromatic C-C bonds.

SEM studies: The surface morphology of bare pencil lead electrode (PLE), graphene oxide nanoparticles (GONPs), PLE electrode modified with GONPs and modified electrode immobilized with urease enzyme evaluated using SEM are shown in Fig. 5a-d.

From the SEM micrographs, the surface morphology of GONPs (~90-120 nm agglomerated NPs) (Fig. 5b) has a characteristic wrinkle and sheet-like structure, which looks like spongy and slender gauze-shaped configuration. The stripped PLE electrode (Fig. 5a) illustrates the flat and dreary morphology, whereas PLE/GONPs electrode (Fig. 5c) revealed spherical, circular and flaky like composition morphology. After immobilizing urease on the surface of PLE/GONPs electrode, the surface morphology altered from sheet-like structure to regular form.

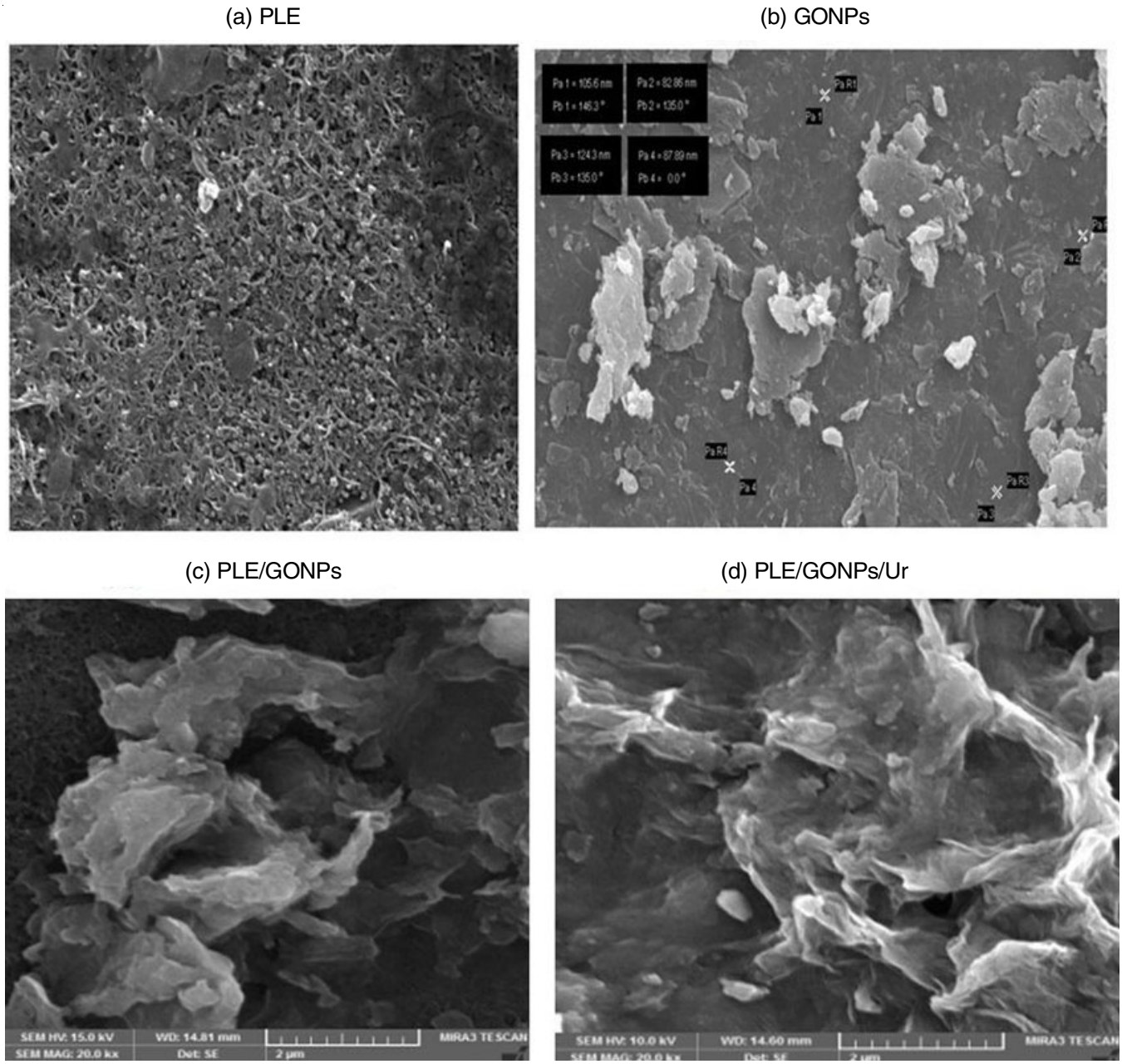

Fig. 5. SEM micrographs of (a) PLE, (b) GONPs, (c) PLE decorated with GONPs (PLE/GONPs) & (d) urease Immobilized PLE/GONPs (PLE/GONPs/Ur)

Cyclic voltammetric studies: Bare PLE, graphene oxide nanoparticles (GONPs) modified PLE and urease immobilized modified PLE were subjected to cyclic voltammetric analysis for examining the change in electrode behaviour after modification and immobilization. The experiment was performed at a scan rate of 0.1 V/s utilizing standard three electrode cell assembly. The electrolytic solution comprised of 1 M KCl dilution containing 3 mM potassium ferric cyanide as redox mediator in boric acid buffer (20 mM). The potential was varied from -0.4 V to 0.4 V with vortex peak 0.410 V. The oxidation and reduction curve obtained is shown in Fig. 6. The results showed that the value of current for the PLE-GONPs electrode was higher than bare PLE. This may be due to the conducting behaviours and higher surface area of graphene oxide nanoparticles [35]. However, after the immobilization of urease enzyme on PLE/GONPs a reduction in the current value was seen compared to the PLE/GONPs electrode, which may be attributed to the insulating behaviour of enzyme which hinders the transfer of electron to the diluted solution and hence confirms the immobilization of urease [36].

Amperometry: The dynamic response amperogram of biosensor electrode *i.e.* PLE and PLE/GONPs/urease was obtained through cyclic voltammetry at different concentrations of urea varying from 0.3-50 mM. The variation was done in a manner to have the concentration of urea doubled in the electrolytic solution at each successive reading. The resulting amperogram are shown in Fig. 7, which revealed that the response obtained for variation in concentration was linear for the range of 0.3-

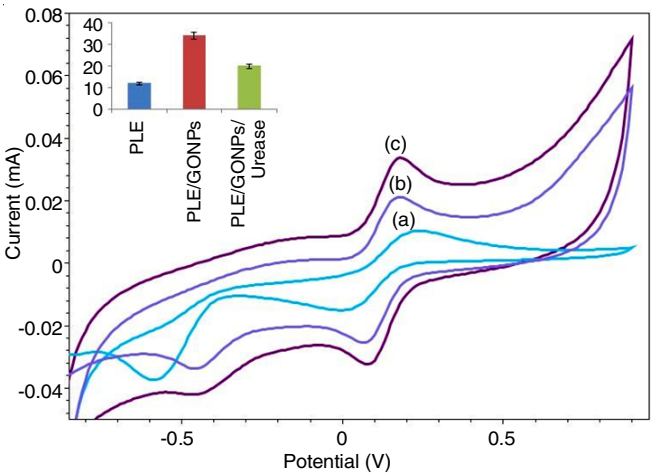

Fig. 6. Cyclic Voltammetry (a) PLE, (b) PLE/GONPs/urease (c) PLE/GONPs

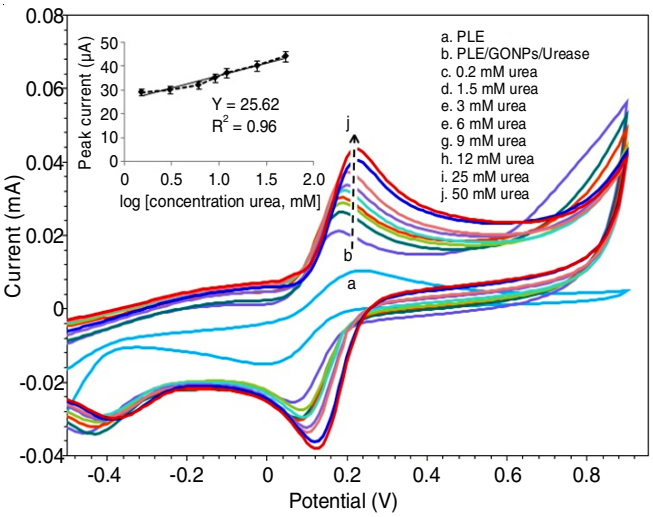

Fig. 7. Cyclic voltammetry (a) PLE, (b) PLE/GONPs/urease at different concentration of urea

50 mM. The sensitivity of the sensing electrode was calculated using slope and crosssectional area and found to be 0.814 μA mM^{-1} cm^{-2}. The modified electrode shows a response time of 5 s.

Comparative studies: Table-1 presented the comparison between the results and analysis reported in other electrochemical sensors with present work. From these results, it can be evidenced that modified electrode has the potential to be commercialized for the detection of urea because of its simplicity, better sensitivity and easy fabrication method.

Conclusion

An improved, low cost and sustainable electrochemical biosensor for urea analysis based on graphene oxide nanoparticles (GONPs) (~90 nm size) decorated over pencil lead electrode (PLE) was prepared. SEM analyses demonstrate that immobilization transformed the GO sheet like structure into regular form. Cyclic voltammetry was performed for examining the performance of PLE and PLE/GONPs/urease electrode. The response of the electrode was linear with a sensitivity of 0.814 μA mM^{-1} cm^{-2} and exhibits a 5 s of response time. The permeable configuration of the GONPs template proffer an incredibly low transfer barrier and consequently endorse quick dispersion of the ionic species commencing to the electrode, responsible for a speedy response time and specifically elevated sensitivity in this work. The simplicity with the cost-effective and superior quality electrochemical presentation holds prospective for the improvement in enzyme immobilized electrochemical biosensors utilized for recognition of urea.

ACKNOWLEDGEMENTS

The authors are thankful to Central Instrumentation Facility, Deenbandhu Chhotu Ram University of Science and Technology, Murthal, India for testing of samples. The authors are also thankful to IIT, Roorkee for providing the SEM facilities.

CONFLICT OF INTEREST

The authors declare that there is no conflict of interests regarding the publication of this article.

REFERENCES

1. P. Bollella and E. Katz, *Sensors*, **20**, 6645 (2020); https://doi.org/10.3390/s20226645
2. I.G. David, D.E. Popa and M. Buleandra, *J. Anal. Methods Chem.*, **2017**, 1 (2017); https://doi.org/10.1155/2017/1905968
3. D.W. Kimmel, G. LeBlanc, M. Meschievitz and D. Cliffel, *Anal. Chem.*, **84**, 685 (2012); https://doi.org/10.1021/ac202878q
4. M.R. Akanda, M. Sohail, M.A. Aziz and A.N. Kawde, *Electroanalysis*, **28**, 408 (2016); https://doi.org/10.1002/elan.201500374

TABLE-1
ASSESSMENT OF THE SENSOR PERFORMANCE WITH OTHER REPORTED ELECTRODES

Electrode	Linear range	Detection limit	Detection method	Sensitivity	Response time	Ref.
ZnPh/GO/Urs on glassy carbon electrode (GCE)	0.4 to 22 μM	0.034 μM	Electrochemical	44.53 μA mM^{-1}	10 s	[18]
Sulfonated graphene/polyaniline nanocomposite (SG-PANI)	0.12-12.3 mM	0.050 mM	Electrochemical	0.85 μA mM^{-1} cm^{-2}	5 s	[24]
Mesoporous silica (SiO_2) embedded graphene oxide (GO)	–	14 mg dL^{-1}	Electrochemical	2.60 μA mM^{-1} cm^{-2}	–	[37]
Manganese oxide-reduced graphene oxide composite	5-100 μM	14.693 μM	Electrochemical	9.70×10^{-3} μA $μM^{-1}$	118 s	[38]
ITO/PDPA/PTA/Gra-ME	1-13 μM	–	Amperometric	1.08 μA $μM^{-1}$ cm^{2}	5 s	[39]
PLE/GO-NPs electrode	0.3-50 mM	0.060 mM	Electrochemical	0.81 μA mM^{-1} cm^{-2}	5 s	Present work

5. K.B. Babitha, P.S. Soorya, A. Peer Mohamed, R.B. Rakhi and S. Ananthakumar, *Mater. Adv.*, **1**, 1939 (2020); https://doi.org/10.1039/D0MA00445F
6. A. Torrinha, N. Jiyane, M. Sabela, K. Bisetty, M.C.B.S.M. Montenegro and A.N. Araújo, *Sci. Rep.*, **10**, 16535 (2020); https://doi.org/10.1038/s41598-020-73635-7
7. H. Beitollahi, S.Z. Mohammadi, M. Safaei and S. Tajik, *Anal. Methods*, **12**, 1547 (2020); https://doi.org/10.1039/C9AY02598G
8. J. Wang, A. Kawde and E. Sahlin, *Analyst*, **125**, 5 (2000); https://doi.org/10.1039/a907364g
9. S. Singh, M. Sharma and G. Singh, *IET Nanobiotechnol.*, **15**, 358 (2021); https://doi.org/10.1049/nbt2.12050
10. S.N. Botewad, D.K. Gaikwad, N.B. Girhe, H.N. Thorat and P.P. Pawar, *Biotechnol. Appl. Biochem.*, (2021); https://doi.org/10.1002/bab.2168
11. M. Hartleb and K. Gutkowski, *World J. Gastroenterol.*, **18**, 3035 (2012); https://doi.org/10.3748/wjg.v18.i24.3035
12. J.C. Chou, C.Y. Wu, S.H. Lin, P.-Y. Kuo, C.-H. Lai, Y.-H. Nien, Y.-X. Wu and T.-Y. Lai, *Sensors*, **19**, 3004 (2019); https://doi.org/10.3390/s19133004
13. R. Vanholder, T. Gryp and G. Glorieux, *Nephrol. Dial. Transplant.*, **33**, 4 (2018); https://doi.org/10.1093/ndt/gfx039
14. D. Grieshaber, R. MacKenzie, J. Vörös and E. Reimhult, *Sensors*, **8**, 1400 (2008); https://doi.org/10.3390/s80314000
15. C.S. Pundir, S. Jakhar and V. Narwal, *Biosens. Bioelectron.*, **123**, 36 (2019); https://doi.org/10.1016/j.bios.2018.09.067
16. C. Zhu, G. Yang, H. Li, D. Du and Y. Lin, *Anal. Chem.*, **87**, 230 (2015); https://doi.org/10.1021/ac5039863
17. G. Zhu, L. Cheng, R. Qi, M. Zhang, J. Zhao, L. Zhu and M. Dong, *Microchim. Acta*, **187**, 72 (2020); https://doi.org/10.1007/s00604-019-4026-0
18. S. Selvarajan, A. Suganthi and M. Rajarajan, *Ultrason. Sonochem.*, **42**, 183 (2018); https://doi.org/10.1016/j.ultsonch.2017.11.030
19. S.N. Botewad, V.G. Pahurkar, G.G. Muley, D.K. Gaikwad, G.A. Bodkhe, M.D. Shirsat and P.P. Pawar, *Front. Mater.*, **7**, 184 (2020); https://doi.org/10.3389/fmats.2020.00184
20. S. Amin, A. Tahira, A. Solangi, V. Beni, J.R. Morante, M. Falhman, X. Liu, R. Mazzaro, Z.H. Ibupoto and A. Vomiero, *RSC Adv.*, **9**, 14443 (2019); https://doi.org/10.1039/C9RA00909D
21. J. Chen, B. Yao, C. Li and G. Shi, *Carbon N.Y.*, **64**, 225 (2013); https://doi.org/10.1016/j.carbon.2013.07.055
22. D.C. Marcano, D.V. Kosynkin, J.M. Berlin, A. Sinitskii, Z. Sun, A. Slesarev, L.B. Alemany, W. Lu and J.M. Tour, *ACS Nano*, **4**, 4806 (2010); https://doi.org/10.1021/nn1006368
23. L. Shahriary and A.A. Athawale, *Int. J. Renew. Energy Environ. Eng.*, **2**, 58 (2014).
24. G. Das, *Int. J. Nanomedicine*, **10**, 55 (2015).
25. M. Nair, S.M. Best and R.E. Cameron, *Appl. Sci.*, **10**, 6911 (2020); https://doi.org/10.3390/app10196911
26. J.Y. Kim, G.Y. Sung and M. Park, *Biomedicines*, **8**, 596 (2020); https://doi.org/10.3390/biomedicines8120596
27. L. Kumar and A. Kaushik, *J. Chem. Pharm. Res.*, **9**, 1 (2017).
28. F.Y. Ban, S.R. Majid, N.M. Huang and H.N. Lim, *Int. J. Electrochem. Sci.*, **7**, 4345 (2012).
29. A. Nepal, G.P. Singh, B.N. Flanders and C.M. Sorensen, *Nanotechnology*, **24**, 245602 (2013); https://doi.org/10.1088/0957-4484/24/24/245602
30. F.T. Thema, M.J. Moloto, E.D. Dikio, N.N. Nyangiwe, L. Kotsedi, M. Maaza and M. Khenfouch, *J. Chem.*, **2013**, 1 (2013); https://doi.org/10.1155/2013/150536
31. W.J. Lin, C.-S. Liao, J.-H. Jhang and Y.-C. Tsai, *Electrochem. Commun.*, **11**, 2153 (2009); https://doi.org/10.1016/j.elecom.2009.09.018
32. K. Pokpas, S. Zbeda, N. Jahed, N. Mohamed and P.G. Baker, *Int. J. Electrochem. Sci.*, **9**, 736 (2014).
33. H.L. Guo, X.F. Wang, Q.Y. Qian, F.-B. Wang and X.-H. Xia, *ACS Nano*, **3**, 2653 (2009); https://doi.org/10.1021/nn900227d
34. A.B. Bourlinos, D. Gournis, D. Petridis, T. Szabó, A. Szeri and I. Dékány, *Langmuir*, **19**, 6050 (2003); https://doi.org/10.1021/la026525h
35. P. Pinyou, V. Blay, K. Chansaenpak and S. Lisnund, *Chemosensors*, **8**, 133 (2020); https://doi.org/10.3390/chemosensors8040133
36. E.N. Waruwu and S. Abd Hakim, *J. Learn. Technol. Phys.*, **1**, 62 (2020); https://doi.org/10.24114/jltp.v1i2.22713
37. S. Abraham, V. Ciobota, S. Srivastava, S.K. Srivastava, R.K. Singh, J. Dellith, B.D. Malhotra, M. Schmitt, J. Popp and A. Srivastava, *Anal. Methods*, **6**, 6711 (2014); https://doi.org/10.1039/C4AY01303D
38. P. Ramasami Sundhar Baabu, M.B. Gumpu, N. Nesakumar, J.B.B. Rayappan and A.J. Kulandaisamy, *Water Air Soil Pollut.*, **231**, 545 (2020); https://doi.org/10.1007/s11270-020-04899-y
39. E. Muthusankar, V.K. Ponnusamy and D. Ragupathy, *Synth. Met.*, **254**, 134 (2019); https://doi.org/10.1016/j.synthmet.2019.06.012